

# Lunar Magnetic Field Observation by MAP-LMAG Onboard SELENE (KAGUYA): Ground and In-orbit Calibration

By Hisayoshi SHIMIZU<sup>1)</sup>, Futoshi TAKAHASHI<sup>2)</sup>, Masaki MATSUSHIMA<sup>2)</sup>,  
Hidetoshi SHIBUYA<sup>3)</sup>, Hideo TSUNAKAWA<sup>2)</sup>

<sup>1)</sup>*Earthquake Research Institute, University of Tokyo, Tokyo, Japan*

<sup>2)</sup>*Department of Earth and Planetary Sciences, Tokyo Institute of Technology, Tokyo, Japan*

<sup>3)</sup>*Department of Earth Sciences, Kumamoto University, Kumamoto, Japan*

A high sensitivity fluxgate Lunar Magnetometer (LMAG) is onboard SELENE (KAGUYA) in order to reveal the near-surface electromagnetic environment and the evolution of the moon through the magnetic field observation. Ground calibration experiments of the LMAG have been performed in order to determine the alignment, sensitivity, and offset of the fluxgate sensor (MGF-S). Orthogonality of the sensors and linearity between the output and ambient magnetic field have been confirmed to fulfill the required accuracy. No clear temperature dependencies of the sensitivity and offset of the sensors were identified within the working temperature in the lunar orbit. The position and orientation of the MGF-S in orbit is monitored by measuring known magnetic field generated by the Sensor Alignment Monitor Coil (SAM-C). The magnetic field distributions by SAM-C were carefully determined by the ground experiments. In-orbit calibration of the orientation of MGF-S using SAM-C have been performed heavily during the initial checkout phase of the satellite and regularly afterwards. Observed stability of the orientation in-orbit is below 0.6 degree. The obtained angles are being used to correct magnetic field data while transforming to coordinate systems such as selenological (ME), GSE and SSE.

**Key Words:** SELENE(KAGUYA), Magnetometer, Calibration

## Nomenclature

**B** : magnetic field  
**r**,  $x, y, z$  : position  
**p**,  $\alpha, \beta, \chi$  : rotation angle  
 $RE$  : radius of Earth

### Subscripts

$x, y, z$  : direction

## 1. Introduction

Magnetic field observations near the moon have been performed occasionally since Apollo 12 in 1969. The purposes of the observations are to understand the evolution and the structure of the moon. For example, existence of magnetic anomalies on the surface of the moon<sup>1)-6)</sup> might imply that the moon had generated magnetic field in the past such as right after the formation of the satellite, although the moon does not have an intrinsic magnetic field at present. Identifying magnetic anomalies and modeling of surface magnetizations, which should be consistent with magnetization mechanisms, on the entire surface of the moon will facilitate the discussion of the lunar evolution. Magnetic field observation also has potential to study the existence of a metallic core of substantial size<sup>7)</sup> and eventually, the origin of the moon and its history thereafter<sup>8)-10)</sup>. The SELENE MAP-LMAG team aims at investigating above mentioned issues by

accumulating magnetic signatures originated from the moon such as the magnetic anomalies on the surface and also by identifying time dependent magnetic responses containing the information on the electrical conductivity of the interior of the moon<sup>11)-15)</sup>.

SELENE is in near polar orbit of about 100 km altitude now as designed. The expected intensity of the signature of the surface magnetic anomalies is 1 nT or less at the altitude. Study of magnetic responses of the moon requires the accuracy of the measurement of order 0.1 nT<sup>11)</sup>. Therefore, designed accuracy of the LMAG observations had set to be less than 0.1 nT.

Designed specifications of the LMAG are shown in Table 1, which are similar to those of the GEOTAIL magnetometer<sup>16)</sup>. The noise level of the ring-core sensors of MGF-S is much less than 0.1 nT. Field measurements can be performed with one of the four ranges but range-0 has been employed for the measurements in the orbit. MGF-S is operating at far end of the 12-meter mast extending from the main body of SELENE to avoid possible electromagnetic noises due to the spacecraft and other scientific instruments. The satellite and all scientific instruments satisfy the electromagnetic compatibility (EMC) conditions which require that the magnetic field due to each of them at the position of MGF-S is less than 0.02 nT. Specification of MGF-S and magnetic environment of SELENE satisfy requirement of lunar magnetic field observation.

Proper ground calibration and in-orbit monitoring of MGF-S is necessary to attain required accuracy of the observation. The zero-offset, sensitivity of each of the fluxgate sensors and relative directions (alignments) among them were determined by the ground calibration. The details of the experiments and results are shown in the next section. Monitoring the alignment of MGF-S with respect to main body of SELENE is essential to have accurate magnetic field vector because the mast, on which MGF-S is installed, may be deformed more or less by thermal expansion or other causes. The alignment monitoring can be done if known field is observable by MGF-S. Because there is no known field in the lunar orbit, SELENE has a Sensor Alignment Monitor Coil System (SAM-C) to generate precisely known magnetic fields. Two linearly independent fields can be generated by a bi-axis coil system of SAM-C. SAM-C is installed at the mounting of the mast, and it produces a magnetic field of about 2 nT at the position of the MGF-S with 2 A electric current.

The spatial distributions of the SAM-C generated magnetic fields have been determined by ground experiments. The details of the experiment and the results are shown in Section 2. The method to determine the orientation of MGF-S is explained in Section 3. The results of in-orbit calibrations of the orientation of MGF-S are shown in Section 3, and comparison of LMAG data with the magnetic field obtained by ACE (Advanced Composition Explorer) is made in Section 4 to show LMAG and in-orbit calibration are working properly.

Table 1. Specification of MGF-S.

sensor	ring core
linearity	better than $10^{-3}$
dynamic range	range-3: +/- 655536 nT range-2: +/- 1024 nT range-1: +/- 256 nT range-0: +/- 64 nT
resolution (16 bit)	range-3: 2.0 nT range-2: 0.03 nT range-1: 0.008 nT range-0: 0.002 nT
noise level	less than 0.1 nT
sampling rate	32 Hz

## 2. Ground Calibration of MGF-S

### 2.1. Sensitivity and alignment

Calibration experiments were conducted in the magnetic test facility in Tsukuba Space Center, NASDA (now, JAXA). A main 3-axis 15 m diameter Braunkopf coil system was used to generate near-zero magnetic field environment. External magnetic field disturbances were cancelled by feedback information from the sub coil system which situated near the main coil system. The total system can achieve magnetic environment of less than 2.5 nT in the 2.3 m diameter spherical space centering the main coil system.

Sensitivity and alignment calibration experiments were

conducted by measuring known magnetic fields by MGF-S<sup>16)-19)</sup>. The known magnetic field is generated by using a 3-axis Helmholtz coil system which can produce a magnetic field within 0.05 nT accuracy in each direction. MGF-S and the Helmholtz coils were aligned accurately using cubic mirrors attached on them and a laser alignment system. The surfaces of the cubic mirrors were orthogonal to each other within 0.1 degrees accuracy, which was the desired accuracy of MGF-S sensors.

Three independent sensor to coil relative directions were employed in order to obtain linearly independent data<sup>16), 20)</sup>. Experiments to determine the sensitivity and alignment of the sensors of MGF-S were done at 20 degrees C temperature. The correlation coefficients of the input and output are larger than 0.999 in each setup and sensor. The sensitivity, summarized in Table 2, is determined within 0.2% error. The relative angles between the sensors are 89.61 (x-y), 89.73 (y-z) and 89.89 (z-x) degrees. The linearity and relative directions between the sensors fulfill the requirement in Table 1.

Table 2. Sensitivity of MGF-S (nT/digit)

	$A_x$	$A_y$	$A_z$
range-3	2.088	2.122	2.086
range-2	0.03681	0.03725	0.03656
range-1	0.00917	0.00932	0.00914
range-0	0.00229	0.00232	0.00228

### 2.2. Temperature dependences of offset and relative sensitivity

Experiments to determine the zero offset, its temperature dependence, and temperature dependence of relative sensitivity (the ratio of sensitivity to the reference sensitivity) were made. To have information about temperature dependencies is essential because the operating temperature of MGF-S in the lunar orbit has been expected to vary from -30 to 30 degrees C, and MGF-S has actually experienced temperature variation in the range between -5 and 25 degrees C in-orbit of the moon.

Zero-offset is in principle determined by making measurement when magnetic field is zero. However, it would not be practical to make and monitor completely zero magnetic field environments. For zero-offset determination, very small magnetic field was measured with four different setups of MGF-S direction. Very small magnetic field environment was attained using a permalloy cylinder placed in the Helmholtz coil system: the cylinder provided shielded space and MGF-S was set in it. The target sensor was aligned in a certain direction to make measurements. The direction of the sensor was both positive and negative, and MGF-S was rotated 180 degrees around the target sensor axis; in total, four measurements for one sensor component were made. The average of the measurements by the four setups is the zero-offset value for the target sensor.

The experiments were done for all the ranges by controlling the temperature stepwise from -35 to 33 degrees C. It is seen that the offset does not depend

systematically on temperature, and the deviation around the average is within 1 nT for range-0, 1 and 2. Averages of the offset for ranges 0 are 0.0 nT, -0.5 nT and -1.7 nT for  $x$ ,  $y$ ,  $z$  sensors, respectively.

Temperature variation of the sensitivity is determined for range-0, which is mainly used for in-orbit observation. In the experiment, -60 nT, 0 nT, and 60 nT of magnetic field was provided in a direction of the coil system. MGF-S was set in a temperature controlled box oblique to the applied field in the direction in which all the component had sufficient sensitivity to the given field. The temperature range was -45 to 32 degrees C. There were no clear systematic temperature dependences of the sensitivity seen in the results. Maximum difference of the sensitivity was about 1.7%. However, the difference of total intensity was less than 0.34%. This implies that some small mechanical movement of MGF-S might have occurred unexpectedly during the experiment such as, for example, a little change of the MGF-S body position in the box. Even though there may be slight temperature dependence, the uncertainty due to the temperature dependence of range-0 sensitivity is of order 0.01 nT for the typical magnetic field of 10 nT. Therefore, we concluded that the temperature dependence of sensitivity is negligibly small for analyses of the lunar magnetic field data. Proper in-orbit calibrations of zero-offset and MGF-S orientation allow us to obtain magnetic field data within 0.05 nT accuracy.

### 3. In-orbit Calibration Using Sensor Alignment Monitor Coil (SAM-C)

#### 3.1. Necessity of in-orbit calibrations

SELENE and LMAG experience large temperature differences due to eclipses. The difference of temperature and/or the effect of sunlight may distort the mast on which MGF-S is installed. Monitoring system of the sensor alignment with respect to the satellite (or satellite coordinate system) is necessary to obtain credible magnetic field data in in-orbit condition. Because the magnetic field in orbit around the moon is usually less than 20 nT, the requirement of the accuracy of the direction determination is not as high as that for the satellite magnetometers for the geomagnetic field observations. By considering the accuracy of the magnetometer (0.05 nT) and the strength of the magnetic field, the required accuracy is of order of 0.1 degrees.

#### 3.2. Sensor Alignment Monitor Coil (SAM-C)

The alignment of MGF-S is monitored by measuring known magnetic field. As there is no well-known ambient natural magnetic field available in the lunar environment, known magnetic fields are applied to MGF-S by the Sensor Alignment Monitor Coil (SAM-C) system on board SELENE for in-orbit calibrations. Note that Cassini has a similar in-flight calibration system called the Science Calibration Subsystem (SCAS).<sup>19)</sup>

SAM-C has two set of coil systems, SAM-C(A) and SAM-C(B), to generate two distributions of linearly independent magnetic fields which are used to determine

the position of the magnetometer, about 12 meters away from the main body of the satellite, and three rotation angles (see Fig. 1). In total six unknowns can be determined simultaneously using the two independent SAM-C magnetic field vector distributions. Multiple measurements in a set of calibration reduce the error of determination of the position and rotation angles. SAM-C generates 1 Hz triangular wave, which continues with the same amplitude for 10 seconds and then decays in 8 seconds, see Fig.2 for the applied electric current. A large number (576) of measurements can be made during one set of measurement with 32 Hz sampling frequency to reduce measurement error. Note that the decaying triangular wave is employed because not only to increase the number of measurements but also to prevent magnetizing the satellite and other instruments by the SAM-C magnetic field.

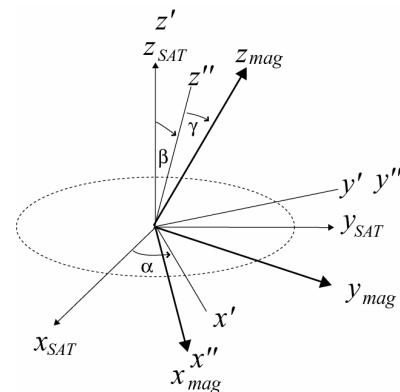


Fig. 1. Definition of the angles of the alignment of MGF-S.

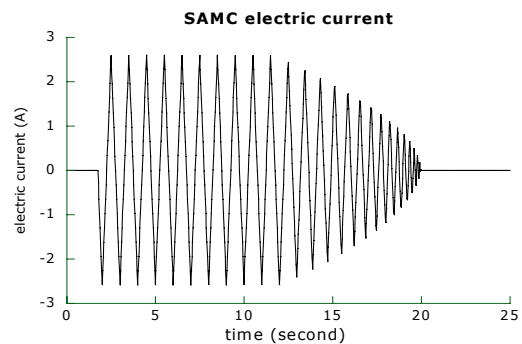


Fig. 2. Example of the variation of SAM-C electric current for in-orbit calibrations

#### 3.3. Distributions of magnetic fields by SAM-C

To determine the distribution of the magnetic field precisely at the position of MGF-S is essential for accurate determination of the rotation angles. Experiments to determine the SAM-C magnetic fields were made in the magnetic test facility at Tsukuba Space Center mentioned in section 2.1. The set-up of the experiment is shown in Fig. 3. SAM-C was placed on a horizontal turn table set in the center of the non-magnetic environment. The magnetic fields generated by SAM-C were measured using 12 fluxgate magnetometers set up as shown in the figure. The orientation of SAM-C in horizontal plane was changed from 0 to 330 degrees by 30-degree steps to increase

effective data of different relative positions of the magnetometers to SAM-C. The electric currents given to the coil system were  $\pm 2.0$  A. Note that the maximum amplitude of the electric currents applied to SAM-C in orbit is 2.6 A.

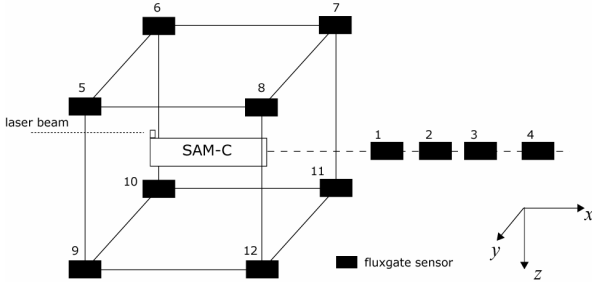


Fig. 3. Arrangement of the magnetometers in SAM-C experiment.

The distribution of the magnetic field is expressed using magnetic potential in spherical coordinate,

$$V = a \sum_{n=1}^N \sum_{m=0}^n \left( g_n^m \cos m\phi + h_n^m \sin m\phi \right) \left( \frac{a}{r} \right)^{n+1} P_n^m(\cos \theta) \quad (1)$$

where  $(r, \theta, \phi)$  represents standard spherical coordinate ( $\theta=0$  coincides with positive  $z$  direction,  $r=0$  is the center of SAM-C),  $a$  is a certain radius, and  $N$  is the truncation degree of the expansion. The determined coefficients  $g_n^m$  and  $h_n^m$  for  $a=2.1$  m and  $N=4$  with 2 A SAM-C electric current are shown in Table 3. The contribution of the terms with  $N>4$  at the position of MGF-S,  $\mathbf{r}_0 = (11.7$  m, 0 m, 0 m) in the  $xyz$  coordinate in Fig.3, is less than 0.01 nT in this case. The magnetic field at the nominal position of MGF-S is, by SAM-C(A),

$$\begin{aligned} B_x &= -1.79 \text{ nT}, & B_y &= 0.00 \text{ nT}, & B_z &= -1.27 \text{ nT}, \\ F &= 2.19 \text{ nT}, \end{aligned} \quad (2)$$

and by SAM-C(B),

$$\begin{aligned} B_x &= 1.93 \text{ nT}, & B_y &= 0.03 \text{ nT}, & B_z &= -1.31 \text{ nT}, \\ F &= 2.33 \text{ nT}. \end{aligned} \quad (3)$$

### 3.4. Linear inversion problem

The alignment angles shown in Fig.1 and the position of MGF-S are determined by a linear inversion. The relationship between the given magnetic field and the observed magnetic field with MGF-S at slightly off from the nominal position  $\mathbf{r} = \mathbf{r}_0 + \Delta \mathbf{r}$  and inclined may be written as,

$$\mathbf{B}_{\text{OBS}}(\mathbf{r}) = \mathbf{R}(\mathbf{p})\mathbf{B}_{\text{SAT}}(\mathbf{r}_0) + \left( \frac{\partial \mathbf{A}}{\partial \mathbf{r}}(\mathbf{r}_0) \mathbf{g} \right) \Delta \mathbf{r} + \left( \frac{\partial \mathbf{A}}{\partial \mathbf{p}}(\mathbf{r}_0) \mathbf{g} \right) \Delta \mathbf{p} \quad (4)$$

where  $\mathbf{p} = (\alpha, \beta, \gamma)$ ,  $\mathbf{g}$  is the vector composed by the Gauss coefficients, the magnetic field at the nominal position is written with matrix  $\mathbf{A}$  as

$$\mathbf{B}_{\text{SAT}}(\mathbf{r}_0) = \mathbf{A}(\mathbf{r}_0) \mathbf{g} \quad (5)$$

and

$$\mathbf{R}(\alpha, \beta, \gamma) = \begin{pmatrix} 1 & 0 & 0 \\ 0 & \cos \gamma & \sin \gamma \\ 0 & -\sin \gamma & \cos \gamma \end{pmatrix} \begin{pmatrix} \cos \beta & 0 & -\sin \beta \\ 0 & 1 & 0 \\ \sin \beta & 0 & \cos \beta \end{pmatrix} \begin{pmatrix} \cos \alpha & \sin \alpha & 0 \\ -\sin \alpha & \cos \alpha & 0 \\ 0 & 0 & 1 \end{pmatrix} \quad (6)$$

Eq.(4) is rewritten as

Table 3. Gauss coefficients to express SAM-C magnetic field.  $a=2.1$  m and  $\pm 2$  A case. Unit is nT.

mode ( $n, m$ )	SAM-C(A)		SAM-C(B)	
	$g_n^m$	$h_n^m$	$g_n^m$	$h_n^m$
(1,0)	223.0395	-	226.5080	-
(1,1)	-155.1038	-0.3778	159.8948	-5.1260
(2,0)	-4.2798	-	5.3552	-
(2,1)	-6.2950	1.3071	3.9018	0.5415
(2,2)	1.2032	-0.7165	-0.5657	0.8414
(3,0)	-4.2728	-	-4.1738	-
(3,1)	-3.9164	0.0298	4.0347	-0.1824
(3,2)	0.9133	-0.0184	0.8367	-0.0123
(3,3)	-1.1781	-0.0031	1.2309	-0.0158
(4,0)	0.3858	-	0.3723	-
(4,1)	-0.0314	-0.0150	-0.0322	0.0785
(4,2)	0.0592	-0.0594	-0.0039	0.0860
(4,3)	-0.0191	-0.0038	0.1400	0.0220
(4,4)	-0.0429	0.0288	0.0369	0.0069

$$\mathbf{B}_{\text{OBS}}(\mathbf{r}) - \mathbf{R}(\mathbf{p})\mathbf{B}_{\text{SAT}}(\mathbf{r}_0) = \begin{pmatrix} \frac{\partial \mathbf{A}}{\partial \mathbf{r}}(\mathbf{r}_0) \mathbf{g} & \vdots & \mathbf{0} \\ \dots & \dots & \dots \\ \mathbf{0} & \vdots & \frac{\partial \mathbf{A}}{\partial \mathbf{p}}(\mathbf{r}_0) \mathbf{g} \end{pmatrix} \begin{pmatrix} \Delta \mathbf{r} \\ \dots \\ \Delta \mathbf{p} \end{pmatrix} \quad (7)$$

The left-hand-side of Eq.(7) is observable and the deviation vectors may be determined.  $\Delta y$  is not determined in calibration because the  $y$  gradient of the SAM-C magnetic field is small. At the nominal position of MGF-S,  $\mathbf{p} = (0, 0, 0)$  and  $\mathbf{r}_0$ , the estimated errors for each component by one set of calibration measurements are, in in-orbit condition (288 measurements are available and electric current is 2.6 A),

$$\Delta x = 4.0 \times 10^{-3} \text{ m}, \quad \Delta z = 1.6 \times 10^{-2} \text{ m}, \quad (8)$$

$$\Delta \alpha = 6.9 \times 10^{-2} \text{ deg}, \quad \Delta \beta = 1.8 \times 10^{-1} \text{ deg}, \quad \Delta \gamma = 1.0 \times 10^{-1} \text{ deg}.$$

Therefore, the direction of MGF-S can be determined with 0.1 degrees accuracy which is sufficient for the magnetic field measurement around the moon.

### 3.5. Results of in-orbit calibration

Calibrations of the MGF-S alignment using SAM-C were made intensively during the initial checkout phase of SELENE scientific operations. The measurements were performed both in the dayside and night side of the moon in order to examine if significant rotation of the magnetic field sensor might happen due to the effect of thermal expansion of some part of the mast.

Fig. 4 shows an example of the observed magnetic field, together with given electric current, during the calibration made on October 29, 2007. The SAM-C generated magnetic field is clearly seen. However, in situ magnetic field, although very quiet at this time, is contained. Also, the wave form is deformed by the effect of induced field due to SAM-C current, especially in  $B_z$ . The time series was processed using a Karman filter and referring to the input electric current in order to separate the SAM-C magnetic field more clearly, see Fig.5. The separated fields have been used to determine the response, the ratio between the observed magnetic field component and applied electric current, and angles of MGF-S.

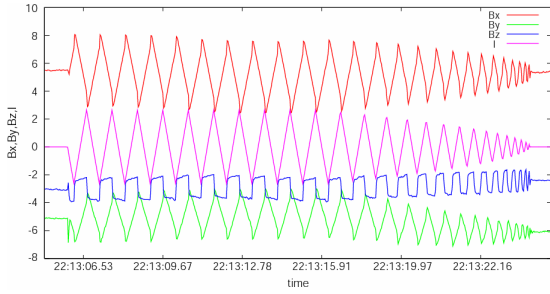


Fig. 4. Calibration time series during quiet magnetic environment..

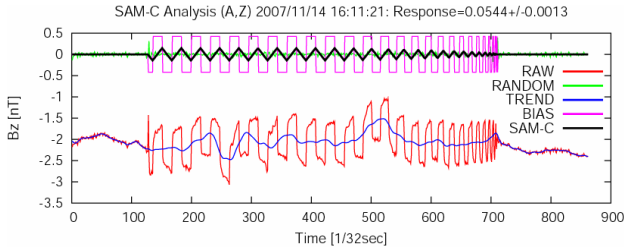


Fig. 5. Observed and processed time series.

Fig. 6 shows all the observed response ( $Y$  component) and temperature during Nov. 5-15, 2007. We may see occasional large deviations of the response from average levels. They are due to large and sub second time scale natural magnetic disturbances, which occur often in the dayside, and do not represent the orientation of MGF-S. See Fig.7 for an example of noisy ambient field and not well determined response (1.19, average=0.60, see Fig.6). If we neglect those ill-determined responses, the responses fall in small range and do not depend on the temperature or the position of the satellite.

The angles determined by in-orbit calibrations are calculated using Eq.(7) and results for calibrations in night side are shown in Fig. 8. If the angles determined by inappropriate data (i.e. those with large and short time scale magnetic disturbances) are removed, the determined angles are within  $\pm 0.5$  degrees range. Note that the angles calculated by well determined dayside response are in the same range. The determined angles are listed in Table 4. The angles are the same within 0.6 degree.

#### 4. Comparison of SELENE/MAP-LMAG and ACE Magnetic Field

Fig. 9 shows time series of the magnetic field observed by SELENE/LMAG and ACE (Advanced Composition Explorer) during November 11-13, 2007. Each of X, Y and Z offsets was basically calibrated using the Davis-Smith method<sup>20)</sup> and the orientation of the sensor determined by in-orbit calibration using SAM-C was applied for data processing. The two satellites are separated by about 230-240 $RE$  during the period. Similar magnetic fields are observed by the two satellites but the arrival times of the signals are 60 minutes later for SELENE. This is due to the propagation of magnetic signature by solar wind. The similarity and time delay of magnetic signature confirm the consistency of the magnetic field observed by ACE and SELENE.

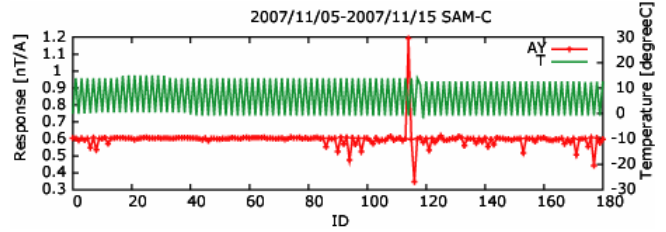


Fig. 6. Observed response ( $Y$ ) for SAM-C(A) and temperature.

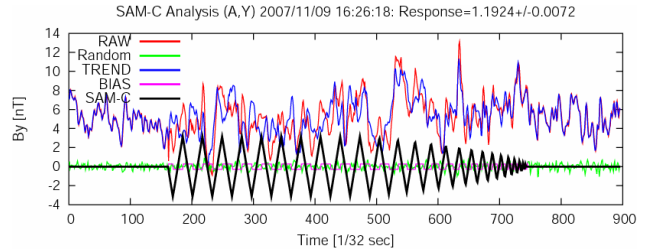


Fig. 7. Calibration record in noisy ambient magnetic field.

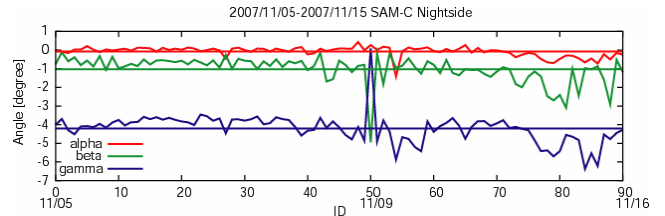


Fig. 8. Rotation angles calculated from response factors.

Table 4. Alignment of MGF-S determined by in-orbit calibrations. Unit is degree.

	$\alpha$	$\beta$	$\gamma$
checkout phase	-0.00	-0.74	-4.01
Feb. 12, 2008	-0.44	-0.34	-3.44

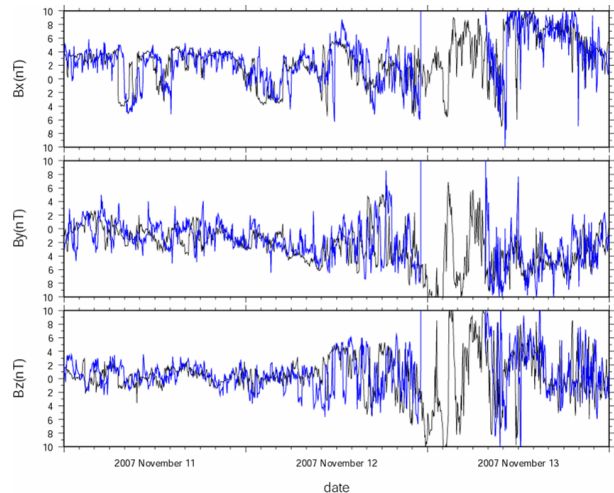


Fig. 9. Observed magnetic field time series by LMAG (blue) and ACE (black) during Nov.11-13, 2007. Coordinate is GSE.

#### 5. Summary

The ground calibration of SELENE magnetometer has been made by a series of experiments. The linearity of the

sensors was confirmed and sensitivity for all ranges was determined. The sensors are orthogonal to each other within 0.4 degree, and further correction can be made using the relative angles of the sensors. The offsets and sensitivities do not show any systematic dependencies on temperature. Thus we conclude that the accuracy of MGF-S is about 0.1 nT. The magnetic field distributions generated by SAM-C, which is used for in-flight calibrations, are determined by the experiments. An electric current of 2 A produces a magnetic field of about 2 nT at the nominal position of the magnetometer, which is about 12 m away from SAM-C. A linear inversion to determine the relative position and alignment of MGF-S was formulated, and it was shown that the estimated error of the angle was of order 0.1 degree.

In-flight calibrations of MGF-S alignment were made intensively during the check-out phase and several times afterwards. No clear temperature dependences of the alignment of MGF-S are seen. The variations of the angles are well within 0.6 degree, which implies that the alignment of MGF-S has been stable in the orbit around the moon.

Comparison of the magnetic field data obtained by ACE and SELENE shows that the MGF-S is working correctly. Also, we can confirm that the zero-offset and orientation of MGF-S have been determined properly by in-flight calibrations. Obtained data are being used for the analysis to obtain magnetic anomaly maps of the moon and to detect induction signature of the moon.

## References

- 1) Hood, L. L., P. J. Coleman, Jr., and D. E. Wilhelms, The moon: sources of the crustal magnetic anomalies, *Science*, 204, 53–57, 1979.
- 2) Hood, L. L. and G. Schubert, Lunar magnetic anomalies and surface optical properties, *Science*, 208, 49–51, 1980.
- 3) Halekas, J. S., D. L. Mitchell, R. P. Lin, S. Frey, L. L. Hood, M. H. Acuña, and A. B. Binder, Mapping of crustal magnetic anomalies on the lunar near side by the Lunar Prospector electron reflectometer, *J. Geophys. Res.*, **106**, 27841–27852, 2001.
- 4) Hood, L. L., A. Zakharian, J. Halekas, D. L. Mitchell, R. P. Lin, M. H. Acuña, and A. B. Binder, Initial mapping and interpretation of lunar crustal magnetic anomalies using Lunar Prospector magnetometer data, *J. Geophys. Res.*, **106**, 27825–27839, 2001.
- 5) Kurata, M., H. Tsunakawa, Y. Saito, H. Shibuya, M. Matsushima, and H. Shimizu, Mini-magnetosphere over the Reiner Gamma magnetic anomaly region on the moon, *Geophys. Res. Lett.*, 32, L24205, doi:10.1029/2005GL024097, 2005.
- 6) Toyoshima, M., H. Shibuya, M. Matsushima, H. Shimizu and H. Tsunakawa, Equivalent source mapping of the lunar crustal magnetic field using ABIC, *Earth Planets Space*, **60**, 365–373, 2008.
- 7) Hood, L. L., D. L. Mitchell, R. P. Lin, M. H. Acuña, and A. B. Binder, Initial measurements of lunar induced magnetic dipole moment using Lunar Prospector magnetometer, *Geophys. Res. Lett.*, **26**, 2327–2330, 1999.
- 8) Richter, K., Does the moon have a metallic core? Constraints from giant impact modeling and siderophile elements, *Icarus*, **158**, 1–13, 2002.
- 9) Lee, D. C., A. N. Halliday, G. A. Snyder, and L. A. Taylor, Age and origin of the moon, *Science*, **278**, 1098–1103, 1997.
- 10) Runcorn, S. K., The formation of the lunar core, *Geochim. Cosmochim. Acta*, **60**, 1205–1208, 1996.
- 11) Dyal, P., C. W. Parkin, and W. D. Daily, Lunar electrical conductivity and magnetic permeability, *Proc. Lunar Sci. Conf. 6th*, 2909–2926, 1975.
- 12) Dyal, P., C.W. Parkin, and W. D. Daily, Structure of the lunar interior from magnetic field measurements, *Proc. Lunar Sci. Conf. 7th*, 3077–3095, 1976
- 13) Russell, C.T., P. J. Coleman, Jr., and B. E. Goldstein, Measurements of the lunar induced magnetic moment in the geomagnetic tail: Evidence for a lunar core?, *Proc. Lunar Planet. Sci. Conf.*, 12, 831–836, 1981.
- 14) Hobbs, B. A., The inverse problem of the moon's electrical conductivity, *Earth Planet. Sci. Lett.*, 17, 380–384, 1973.
- 15) Hood, L. L., F. Herbert, and C. P. Sonett, The deep lunar electrical conductivity profile: Structural and thermal inferences, *J. Geophys. Res.*, **87**, 5311–5326, 1982.
- 16) Yamamoto, T., S. Kokubun, and GEOTAIL/PLANET-B MGF Team, Ground calibration of high-sensitivity magnetometers for spacecraft use, *Uchu Kagaku Kenkyuusho Houkoku*, **88**, 1–24, 1996.
- 17) Lohr, D. A., L. J. Zanetti, B. J. Anderson, T. A. Potemra, J. R. Hayes, R. E. Gold, R. M. Henshaw, F. F. Mobrey, and D. B. Holland, NEAR magnetic field investigation, instrumentation, spacecraft magnetic and data access, *Space Science Rev.*, **82**, 225–281, 1997.
- 18) Risbo, T., P. Brauer, J. M. G. Merayo, O. V. Nielsen, J. R. Petersen, F. Prindahl, and I. Richter, Oersted pre-flight magnetometer calibration mission, *Meas. Sci. Technol.*, **14**, 674–688, 2003.
- 19) Dougherty, M. K., S. Kellock, D. J. Southwood, A. Balogh, E. J. Smith, B. T. Tsurutani, B. Gerlach, K.-H. Glassmeier, F. Gleim, C. T. Russell, G. Erdos, F. M. Neubauer, and S. W. H. Cowley, The Cassini magnetic field investigation, *Space Science Rev.*, **114**, 331–383, 2004.
- 20) Davis, L. jr., E. J. Smith and J. Belcher, The In-Flight Determination of Spacecraft Magnetic Field Zeros, *Trans. AGU*, **49**, 257, 1968.